Slovak Geol. Mag., 8, 3– 4 (2002), 179 – 193

Ore mineralization on the Pezinok – Trojárová deposit in the Malé Karpaty Mts., Slovakia: mineralogical and geochemical characterization

MARTIN CHOVAN[1], STANISLAVA TRTÍKOVÁ [2], VOJTECH VILINOVIČ[3], MILOŠ KHUN[4], PETER HANAS[5]

[1]Dept. of Mineralogy and Petrology, Faculty of Natural Sciences, Comenius University, Mlynská dolina G, 842 15 Bratislava
[2]Geological Institute, Slovak Academy of Sciences, Severná 5, 974 01 Banská Bystrica
[3]GEOTEST Bratislava, Ltd., Vlčie hrdlo, 821 07 Bratislava.
[4]Dept. of Geochemistry, Faculty of Natural Sciences, Comenius University, Mlynská Dolina G, 842 15 Bratislava
[5]Slovak Ministry of Environment, Nám. Ľ. Štúra 1, 812 35 Bratislava.

Abstract: Ore mineralization on the Trojárová deposit is hosted in metamorphosed black shales, embraced by complex of metabasics and metatuffs. Following ore mineralizations were discerned: 1) metamorphosed exhalation-sedimentary pyrite mineralization, 2) molybdenite mineralization in granitoides; and 3) hydrothermal Sb-Fe-As-Au mineralization. Geochemical investigation of ore bearing black shales revealed intensive pyritization of black shales, close association of Sb-Fe-As-Au sulphidic mineralization with carbonates and Au binding to arsenopyrite. Five successive stages of hydrothermal Sb-Fe-As-Au mineralization were distinguished, with stibnite mineralization in 3rd and 4th stage. Main factor controlling the stibnite deposition was probably the decreasing temperature.

Key words: black shales, carbonatization, arsenopyrite, stibnite

Introduction

The Trojárová locality is situated northwards from Sb-Au deposit Kolársky vrch in one of productive zones of larger area between the towns Pezinok and Pernek in Malé Karpaty Mts. (Fig. 1). Positive geochemical anomalies were detected in exploration boreholes and subsequently the Trojárová adit was drilled in order to investigate the Au-As and Sb mineralizations. This study summarizes main results of detailed mineralogical, petrological and geochemical research performed on samples from the drillcores and from the Trojárová adit.

Geological setting and ore mineralization

Variscan crystalline in surroundings of studied area consists of two granitoid bodies (southern Bratislava massive and northern Modra massive) and a zone of metamorphites inbetween, stretching in the NW-SE direction across the mountain ridge (Pezinok-Pernek crystalline). Three lithologic units were recognized in the metamorphic belt (Pezinok, Pernek and Harmónia succession), each one composed of two formations. Lower pelitic-psamitic flysch-like formation of silurian–lower devonian age gradually passes into upper volcanosedimantary formation of lower–middle devonian age (Planderová & Pahr, 1983) with black shales, basalts and basaltic tuffs, carbonates, gabros and gabbrodiorites. Intrusives of the Bratislava massive are represented by peraluminous monzogranites and granodiorites with high quartz contents (Cambel & Vilinovič, 1987) classified as Ca-alkaline granitoids to granites. Modra granitoids are shifted towards Ca-alkaline-trondhjemitic series, represented by metaaluminous-peraluminous biotitic granodiorites and tonalites. Both granitoid massives exhibit Rb-Sr age 348 ±4 Ma (Cambel et al., 1990). Putiš (1987) and Plašienka et al. (1991) distinguished four stages of variscan tectonometamorphic evolution of related area:

1. regional metamorphism;
2. peripluthonic metamorphism with distinctive zonality, related to intruding of the Bratislava massive;
3. contact metamorphism caused by the intrusion of Modra massive
4. late variscian fold tectonics of the metamorphic belt between the towns Pezinok and Pernek.

Alpine evolution of studied area started by epivariscan clastic sedimentation in upper permian and evolved through different tectonic regimes (rifting – areal extension – pre-compressional subsidence – compression; each accompanied by its characteristic sedimentation) to the thrusting and nappe emplacement, which took place in middle Cretaceous and determined the present day geological structure of Malé Karpaty Mts. Neogene brittle tectonics has slightly rearranged this paleoalpine structure and caused uplift of the horst of present-day mountain ridge along major normal- and strike-slip faults.

The ore mineralizations in Malé Karpaty Mts. were subject of numerous studies, among others Cambel (1959), Polák (1974), Kantor (1974), Žákovský (1962), Andráš (1984). Reader could find good review in Chovan et al. (1992), who distinguished the following mineralization types in four productive zones in the Malé Karpaty Mts. crystalline:

I. Metamorphosed exhalation-sedimentary mineralization with pyrite;

II. Hydrothermal mineralization, with following subtypes: 1. – molybdenum in granitoids; 2. – copper-base

Geological Survey of Slovak Republic, Dionýz Štúr Publishers, Bratislava 2002 ISSN 1335-96X

Slovak Geol. Mag., 8, 3–4 (2002), 179 – 193

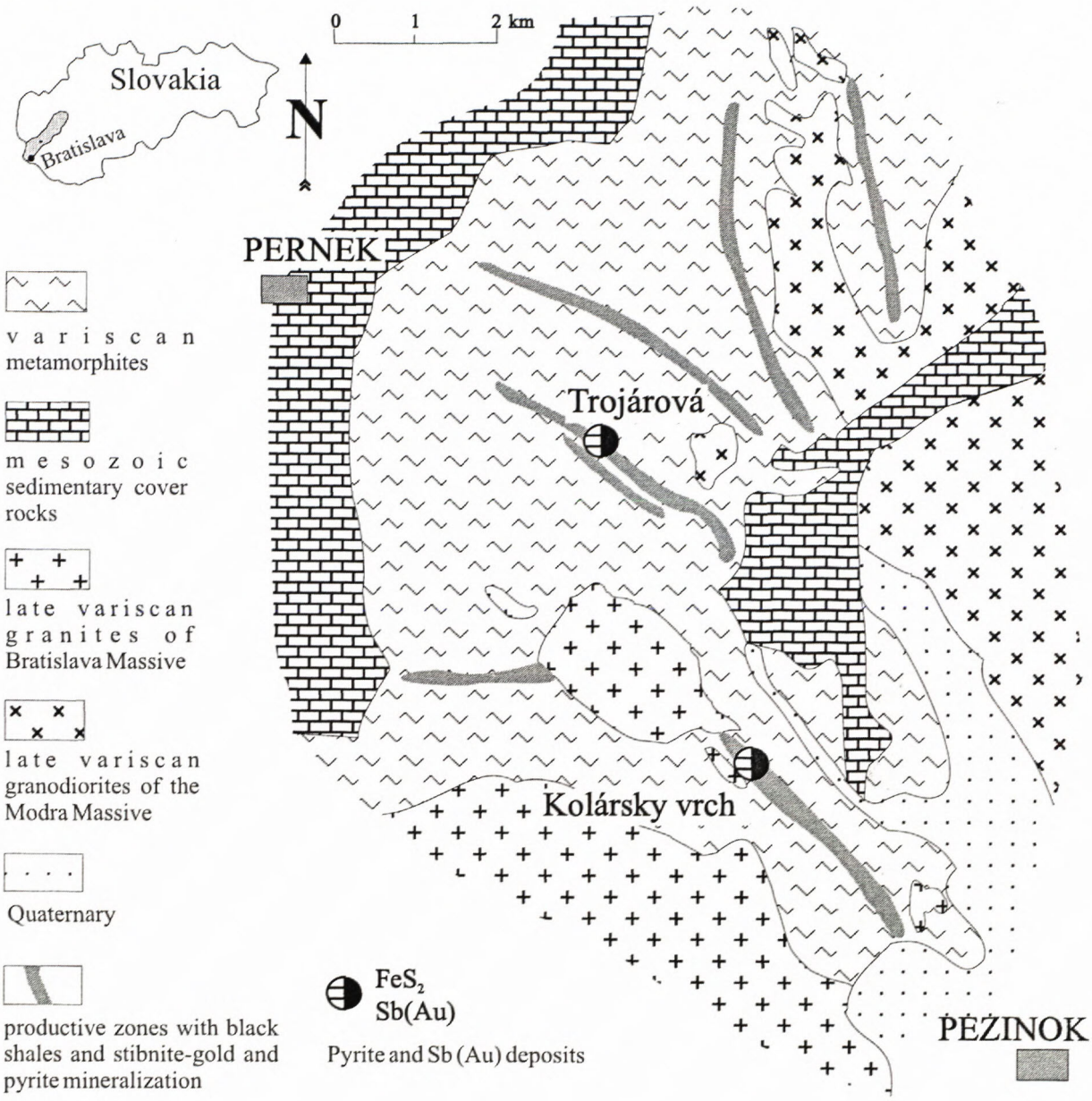

Fig. 1 Simplified geological map of the Malé Karpaty Mts., region between Pezinok and Pernek (after Cambel 1959; Polák & Rak 1980).

III. metal with silver: (a) Cu-Pb, Ag, (Ni); (b) Pb-Zn; (c) Pb-Ag; 3. – antimony-gold: (a) gold-sulphidic; (b) gold-quartz; (c) stibnite.

Sampling and analytical methods

The material for mineralogical, petrological and geochemical study was obtained from the cores of exploratory boreholes and from the prospection adit on Trojárová locality. Several samples of nearly identical mineralization from adit Antimonitová (Kolársky vrch deposit) were collected for comparison.

Optical microscopic observations were carried out on the microscope Jenapol. Electron WDS microanalyses were performed on JEOL, JXA 840 A (Faculty of Natural Sciences, Comenius University) (analyst Krištín) and by JEOL SUPERPROBE 733 (Geological Survey of Slovak Republic), accelerating voltage 20 KeV, 15 nA, beam diameter 5.10^{-6} m, standards Sb_2S_3, GaAs, FeS_2, FeAsS, HgS-Hg, PbS-Pb, Ag, Sb, Zn, Cu, Bi, Co, Ni, Au, Mn a Cd (analysts Caňo and Siman). Semiquantitative EDS and scanning electron microprobe images were performed by JSM 840 (Geological Survey of Slovak Republic).

Following spectral analytical methods were used to determine the concentrations of individual elements (laboratories of Geological Institute of Faculty of Natural Sciences, Comenius University, and Institute of Geological Exploration in Spišská Nová Ves): Au - AAS; As and Sb - AAS with hydride generation technique; trace elements – OES; C_{org} and C_{min} quantitative analysis. AAS analyses of Au were performed by Philips PU 9000 with deuterium background corrector using electrothermic

atomization PV 9095 Video Furnace in Ar atmosphere (Geological Institute of Slovak Academy of Sciences, Banská Bystrica). Manometric, thermometric analysis and X-ray powder diffraction analysis were carried out in Geological Institute of Faculty of Natural Sciences, Comenius University.

The samples of black shales from cores of boreholes PT-13, PT-55, PT-57 were studied by means of Infrared Absorption Spectroscopy where Soxhlet's method was applied for organic component extraction and method of column chromatography for organic material fractionation. The contents of C, H, N, S was determinated by Element Analyser Carlo Erba 1106 (Department of Organic Chemistry, Faculty of Natural Sciences Comenius University). Chemical separation of graphite was performed in the laboratory of analytical chemistry (Geological Survey of Slovak Republic). Contents of trace and metal elements in bulk samples was determinated by means of quantitative SPA and AAS (Geological Institute of Faculty of Natural Sciences Comenius University). The contents of P_2O_5 was estimated photocolorimetrically (Dept. of Economic Geology, Faculty of Natural Sciences, Comenius University).

Results

Surrounding rocks

The black shales form narrow strips within the "belts" of actinolitic schists. These are embraced by amphibolites. This complex is underlain by by staurolite-biotite paragneisses and granitoids of the Bratislava massive. Their contact is accompanied by a cataclastic zone of thickness up to 2 m.

"Actinolitic" schists exhibit prevailingly nematoblastic structure. Their ground mass consists of collumnar to spicular "actinolite", chlorite, quartz and sphene. According to classification of Leake et al. (1997) the previously mentioned actinolite corresponds to Mg-hornblendite – tchermakite (Moravanský et al., 2001). Carbonates, pyrite and "actinolite" are arranged into coarse-grained layers. Heterogranular porfyroblastic texture and granonematoblastic texture with blasts of plagioclase and quartz occurs sporadically. A graphitic substance is present in zones adjacent to the black shales, which indicates gradual transitions between the two lithotypes. This is well documented by presence of the amphibole in black shales.

Amphibolites are characterized by heterogranular porphyroblastic texture, their matrix is composed of amphiboles, finegrained light sphene, pyrite and carbonates. Blasts of plagioclase, carbonate, "actinolite", quartz and minerals of epidote-zoisite group occur in this matrix.

Tectonic breccias occur on the contact of the complex of metabasites and granitoid rocks and were formed mostly on the expense of granitoids. Their textures indicate transition between mylonitization and brittle cataclasis. The observations in our material are in agreement with the concept of Putiš (1987) about the overthrust of metabasite complex over the paragneisses.

Granitoid rocks are affected by cataclasis / mylonitization, which is mostly localized at the contact with metabasites.

Staurolite-biotite paragneiss are affected by regional-periplutonic metamorphism (staurolite-sillimanite zone) caused by the intrusion of granitoids (Korikovskij et al., 1984).

Hydrothermal alterations

Moravanský (2000) distinguished three alteration zones: carbonitization and illitization zone, muscovitization zone and chloritization zone. The altered rock is characteristic by the association carbonate-sericite-quartz-pyrite. "Actinolitic" schists are affected by carbonatization, which is most intense at their contact with black shales and it fades out with the distance from the contact. Carbonatization is localized 1) in the foliation; and 2) in veins cutting the foliation, filled by carbonates, quartz, ±albite and ore minerals.

Hydrothermal alterations of granitoids comprise sericitization and in lesser extent carbonatization of plagioclases, muscovitization and chloritization (Moravanský, 2000; Moravanský et al., 2001).

Ti-Fe oxides in hydrothermally altered black and actinolithic shales form anhedral grains with low reflectance, arranged concordantly with foliation.

V-Cr garnet was recorded in actinolithic-tremolitic schists on the localities Trojárová and Rybníček (Uher et al., 1994).

Black shales

Ore mineralization is hosted in the black shales which form zones with thickness up to 20 m in the actinolitic schists (Fig. 2). Their weak rheology designated them to deform much more intensively than surrounding rock during orogenic processes, which is pronounced in subtly-folded structure. Black shales consist of quartz, sericitic matrix, organic matter and biotite of two generations. Plagioclase, chlorites, carbonates, actinolite, Ti-oxides(?), rutile and apatite occurs as accessory minerals. Black shales are impregnated with pyrite, arsenopyrite is rare.

The average contents of C_{org} in black shales is 5.5 %. Infrared spectra of organic compounds extracted in benzene show for occurrence of absorption bands which are assigned to valence vibrations of C-H bands of CH_3, CH_2, or CH groups. The C-O-C bands in esteric and etheric compound and C=O bands of saturated kethon and unsaturated ester of karboxylum acid are abundant. Two samples were analysed for contents of H, C and S, following results were obtained: H – 10-0.30 %; C – 5.46-5.48 %; S – 5.95-7.82 % (Oružinský et al., 1990).

The samples from boreholes and adits were analysed for contents of accessory and trace elements, whereby enrichment in S_{tot}, C_{org}, C_{min}, Sb, Au, and As compared to surrounding rocks was revealed (Fig. 3). Contents of Au, As and Sb represent significant anomaly (sensu Judovič et al., 1990; Judovič & Kertis, 1991). From comparison of these values with those from other black shales productive zones of Malé Karpaty Mts. (Cambel & Khun, 1983) follows 4.9x enrichment for Au, 38.7x for Sb and 21.2x for As.

Remarkably high contents of Mo in the samples from boreholes are presumably connected with greisenized granitoids with molybdenite in the underlier. An increased contents of V in black shales samples was determined too.

Slovak Geol. Mag., 8, 3–4 (2002), 179 – 193

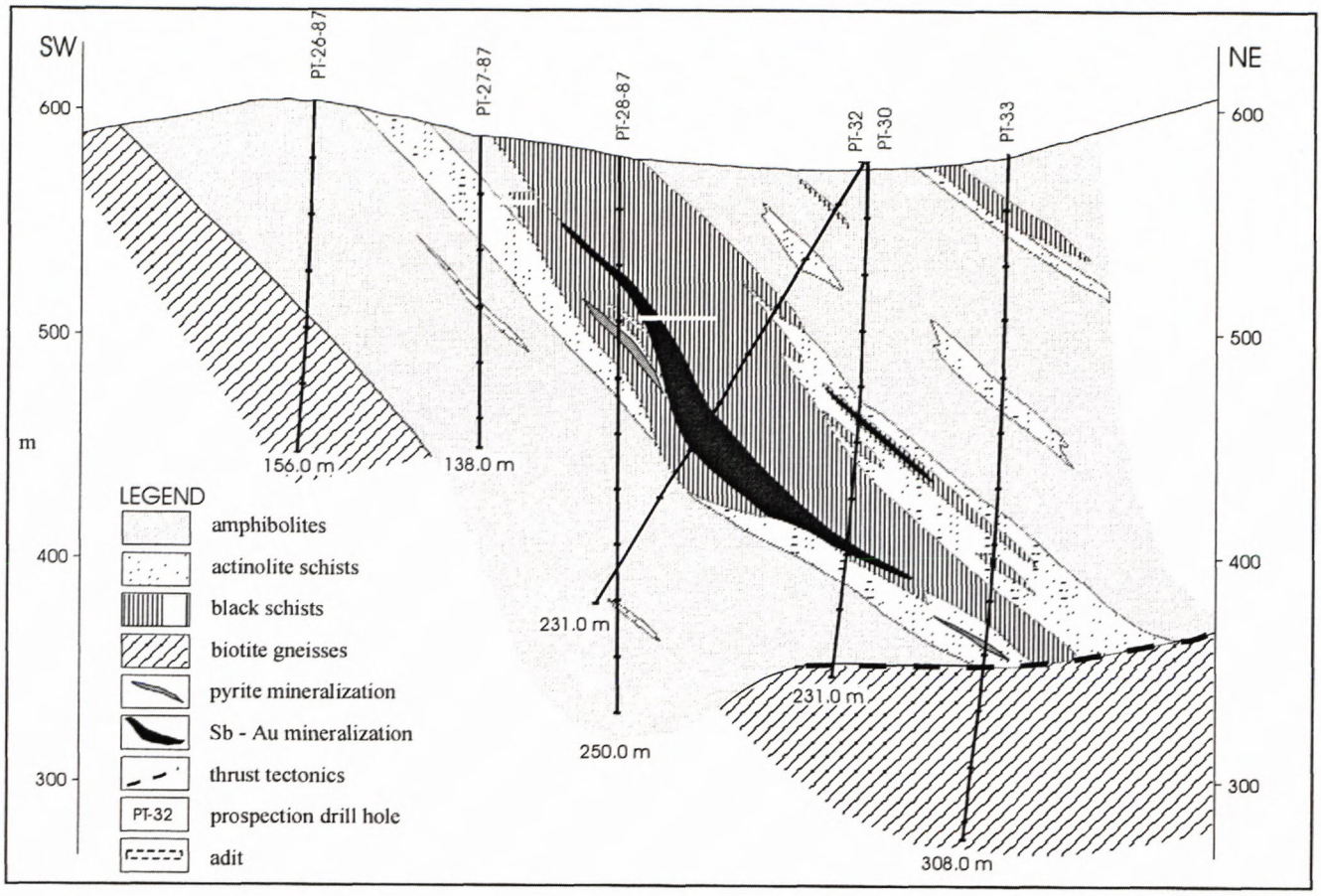

Fig. 2 Geological profile across the complex of crystalline schists with position of boreholes and prospection adits on the Trojárová deposit, Malé Karpaty Mts. (after Hanas et al., 1989).

An Sb and arsenopyrite mineralization was detected in black shales from boreholes on the Trojárová locality. Negative correlation between C_{org} and C_{min} (r = -0.661) follows from the statistical analysis of geochemical data from these samples, affinities of other elements to C_{org} are as follows: V 0.799; Zr 0.724; Y 0.69; Ni 0.656; Sb 0.589, indistinct positive correlations show Pb, Mo, Cu, and Ag. Sr (0.706), Sc (0.67), and Cr (0.606) have significant positive correlation with C_{min}. V (-0.717), Ni (-0.569), Cu (-0.498), Mo (-0.498) (Fig.4) show negative correlation with C_{min}. Elements Co, Ba, Bi, and B have very weak positive correlation with both C_{org} and C_{min}. The contents of As, Au, and S_{tot} were not determined in the borehole samples. These correlation coefficients are in compliance with other published data from black shales (e.g. Judovič & Kertis, 1991).

The fully evolved Sb-Fe-As-Au mineralization (see below) proved in boreholes was not attained during the exploration works in the Trojárová adit, and drilling stopped in its marginal zone. Therefore arsenopyrite and pyrite are dominant here and Sb-minerals occur in accessory amounts. Studied samples of this mineralization exhibit affinity of Au, As and Sb to C_{min} (0.847, 0.617 and 0.519, respectively) (Fig. 5). This indicates the correlation of these elements with the intensity of carbonatization. Correlation of S_{tot} with C_{org} (0.526) shows for synsedimentary pyritization in black shales. Arsenic has a negative correlation with C_{org} (-0.593). Close association of Au and As (0.703) is related to Au-enrichment in arsenopyrite which is bound to carbonatic layers in black shales. Sb positive correlation with Au and As can point to the presence of an Au alloy in Au bearing arsenopyrite.

Graphite was identified and investigated in several samples from boreholes. Those samples were grinded and treated by chemical agents - carbonates were removed in HCl (by 60°C), silicates in HF (60°C), fluorides by powdered Zn after mechanical processing (see Janků, 1991). Separated graphite exhibits slice morphology, euhedral grains are scarce (Fig. 6). Grain size ranges up to 10 μm (Fig. 6), exceptionally up to 50 μm, which ranks the studied samples to microcrystalline graphite (1 μm - 100 μm). Value of *c*-parameter, calculated from the *d(001)* spacing of X-ray diffraction patterns (Tab.1) of graphite is 6.735 x 10^{-10}m.

Ore mineralization

Three mineralization types were distinguished on the Trojárová locality:

1. metamorphosed pyrite-pyrrhotite Fe-S mineralization of volcano-sedimentary origin,
2. molybdenite mineralization,
3. hydrothermal Sb-Fe-As-Au mineralization.

Fe-S mineralization

Mineralization is hosted in amphibolite layers, "actinolitic" schists and black shales.

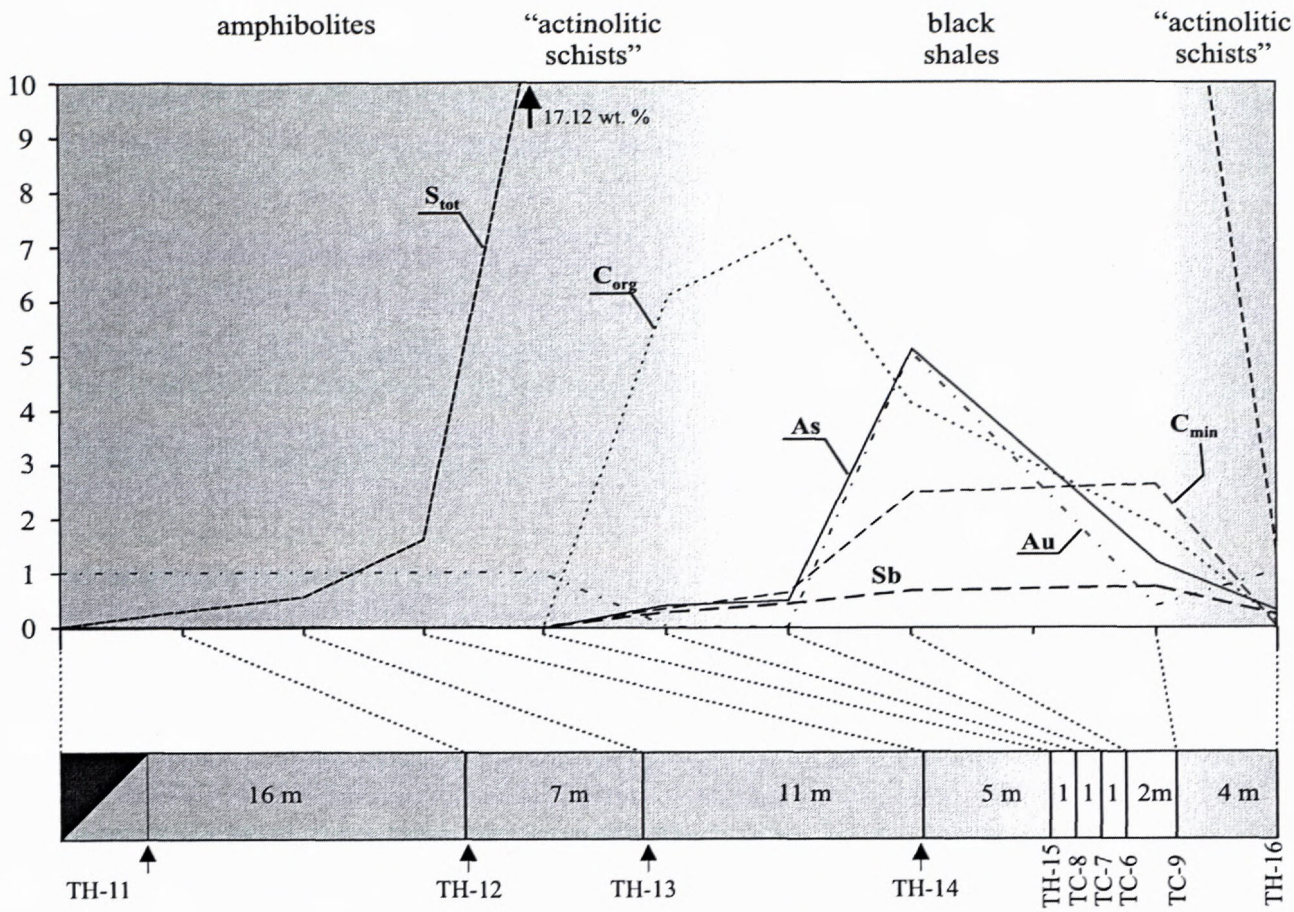

Fig. 3 Schematic profile of PT5 gallery in the Trojárová adit with plot of S_{tot}, C_{org}, C_{min}, Sb, As, and Au contents in amphibolites, actinolitic schists and black shales. Strong increase in contents of these elements is bound to black shales. The contents of Au in ppm x 10, contents of S_{tot}, C_{org}, C_{min} in wt.%, Sb and As content in wt.% x 10. Position of sampling sites TH11-TH16 and TC6-TC9 is shown on the bottom of the picture.

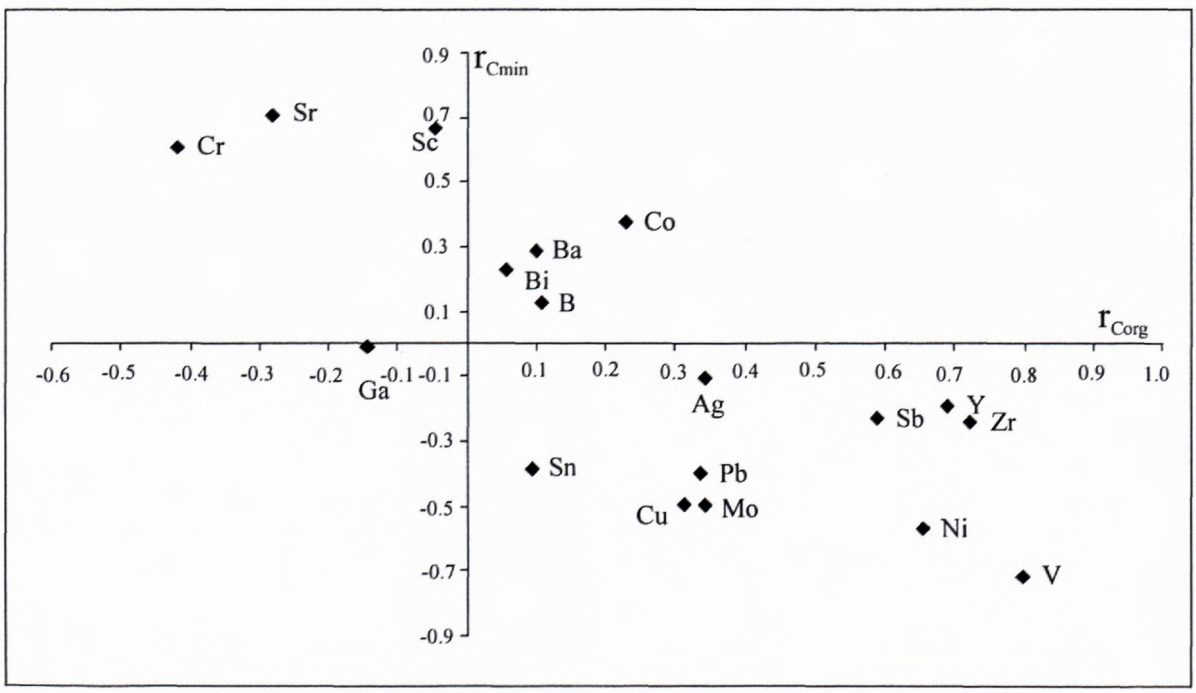

Fig. 4 Plot of correlation coefficients of analysed elements in black shales from boreholes (12 samples), r_{Corg} and r_{Cmin} are correlation coefficients of C_{org} and C_{min} with corresponding elements.

Slovak Geol. Mag., 8, 3–4 (2002), 179 – 193

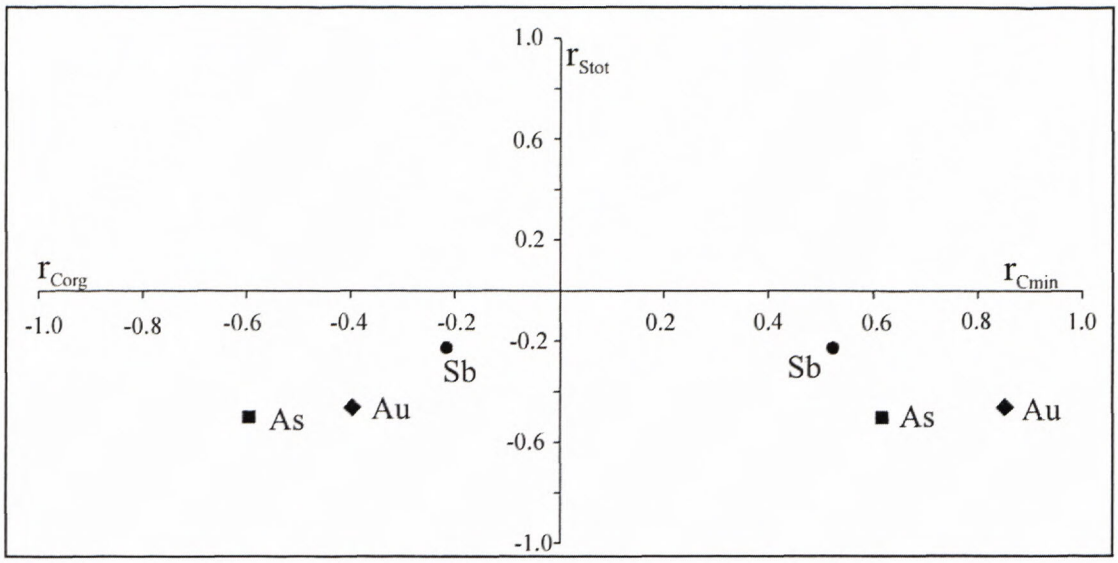

Fig. 5 Plot of correlation coefficients of As, Au, and Sb in black shales samples from Trojárová adit (14 samples), r_{Stot}, r_{Corg}, r_{Cmin} are correlation coefficients of S_{tot}, C_{org}, and C_{min} with corresponding metal elements.

Tab. 1 X-ray diffraction data of graphite from Trojárová black shales (Janků, 1991).

dm sample7	I/Imax	dtab graphite	I graphite	hkl	d pyrite	I pyrite	d arsenopyrite	I arsenopyrite
3.85	15	-	-	-	-	-	-	-
3.351	**100**	**3.36**	**100**	002	-	-	-	-
3.22	5	-	-	-	-	-	-	-
3.121	10	-	-	-	3.128	35	-	-
2.998	10	-	-	-	-	-	-	-
2.965	5	-	-	-	-	-	-	-
2.706	20	-	-	-	2.709	85	-	-
2.423	20	-	-	-	2.423	65	2.418	95
2.212	15	-	-	-	2.219	50	2.204	25
2.112	5	2.13	10	100	-	-	-	-
1.914	15	2.03	50	101	1.915	40	1.943	25
1.813	8	1.80	5	102	-	-	1.814	90
1.758	5	-	-	-	-	-	1.759	20
1.687	10	1.678	80	004	-	-	-	-
1.631	30	-	-	-	1.633	100	1.631	30
1.502	5	1.544	10	103	1.5025	-	-	-
1.450	5	-	-	-	1.445	25	-	-

Pyrite (Tab. 2, analyses 1, 2) as dominant mineral of this mineralization forms impregnations, layers and thin lenses arranged concondantly with foliation. Usually it forms anhedral grains and their aggregates, often intensively corroded and cataclassed (Fig. 7). In fine grained aggregates pyrite also occurs in intergrowths with quartz and pyrrhotite. Mineralization was metamorphosed and intensively folded, whereby the new generation of recrystallized pyrite originated.

Pyrrhotite is abundant mineral and probably represents product of metamorphism of pyrite mineralization. (Tab. 2, analyses 3, 4)

Chalcopyrite is rare, it forms anhedral grains in pyrrhotite aggregates (Tab. 2, analysis 5).

Sphalerite occurs frequently but in small amounts in the form of tiny grains in pyrite-pyrrhotite aggregates. Its increased contents of Fe - 7.9 wt.% average is notable (Tab. 2, analysis 6).

Mo mineralization

A molybdenite specimen of size 3x3 cm was found in the drillhole PT 45 in depth 271 m (Hanas et al., 1989) in almost monomineral muscovite rock of greizen appearance (Fig. 8). Its host rock - muscovitic leucogranite – forms the underlier of the complex of metatuffs and metabasites. From geochemical viewpoint molybdenite is pure, almost without admixtures (Tab. 5, analysis 1). Thermoelectric voltage measurements revealed the P-type conduction (hole type), values of thermoelectric voltage coefficient are typical for molybdenite from greizens (Ďurža & Chovan, 1995).

Sb-Fe-As-Au mineralization

Carbonate and quartz veins with hydrothermal Sb-Fe-As-Au mineralization are hosted in the black shales.

Tab. 2 Electron microprobe analyses of minerals of pyrite-pyrrhotite mineralization (wt. %), the Pezinok – Trojárová deposit, pyrite (1,2), pyrrhotite (3,4), chalcopyrite (5), sphalerite (6).

Analyse num.	1	2	3	4	5	6
Sample	45/9	45/9	45/9	45/9	45/9	45/9
Fe	47.11	47.78	60.14	58.17	30.42	7.85
Bi	-	-	-	0.00	-	0.19
S	51. 05	55.42	39.04	39.72	35.44	32.91
As	0.34	0.03	0.01	-	0.00	-
Ni	0.08	0.07	0.42	-	0.03	-
Co	0.08	0.09	0.07	-	0.03	-
Cu	0.03	0.03	0.00	-	34.13	-
Zn	-	-	-	0.38	-	59.17
Hg	-	-	-	0.32	-	0.00
Mn	-	-	-	0.00	-	0.06
Cd	-	-	-	0.04	-	0.38
Ag	-	-	-	0.02	-	0.00
Σ	98.69	99.04	99.68	98.65	100.05	100.56
recaltulated on the Σ of atoms						
	3	3	2	2	4	2
Fe	1.04	0.99	0.94	0.91	1.00	0.14
Bi	-	0.00	-	0.00	-	0.00
S	1.95	2.00	1.06	1.08	2.02	0.99
As	0.01	-	0.00	-	0.00	-
Ni	0.00	-	0.01	-	0.00	-
Co	0.00	-	0.00	-	0.00	-
Cu	0.00	-	0.00	-	0.98	-
Zn	-	0.00	-	0.01	-	0.87
Hg	-	0.00	-	0.00	-	0.00
Cd	-	0.00	-	0.00	-	0.00
Ag	-	0.00	-	0.00	-	0.00

Arsenopyrite is the m ost abundant ore mineral in the Trojárová adit. It forms crystallic aggregates in carbonate-quartz lenses and veins in black shales, in minor extent also in carbonate veins in actinolitic shists adjacent to black shales. Arsenopyrite treats in two morphological types:

1. The enhedral, severely cataclased arsenopyrite forms crystalline aggregates with grainsize ranging from <10 μm to 100 μm (samples: T-24, T-39, T-40, Tab. 3, analyses 1 to 7). It often intergrows with coarse-grained pyrite. The sectional zonality due to the irregular distribution of Sb (bright zones) and As in arsenopyrite grains is shown on SEM images (Fig. 9). Grains with exceptionally high Au concentration up to 6700 ppm occur in T-24 sample, (Tab. 3, analyses 1 to 4).
2. Euhedral (sometimes subhedral) arsenopyrite forms crystallic aggregates and isolated crystals of size up to 150 μm in carbonate and quartz. The inner grain texture is heterogenous, oscillatory zonation is frequent (Fig. 10). The alternation of bright and dark zones is again related to differences in As and Sb distribution. Arsenopyrite with diffuse zonality occurs rarely (sample T-20). Increased contents of Au was scarcely detected in several grains by means of electron microprobe (up to 800 ppm, Tab. 3, analysis 8).

According to electron microanalyses arsenopyrite has high contents of S, decreased contents of As and adequate contents of Fe - $Fe_{1.005}As_{0.85}S_{1.135}$ considering theoretical arsenopyrite composition. Contents of As is 27 at. % in average, which is too low for implementation of the Kretschmar & Scott´s (1976) arsenopyrite thermometer. As is replaced by Sb in samples where value of correlation coefficient is -0.8. Younger carbonatic veins with Sb mineralization leak into this arsenopyrite mineralization. Arsenopyrite is replaced by stibnite and it contains extremely Sb rich zones with contents of Sb up to 11 wt. %.

Besides these two types some other arsenopyrite morphological varieties were discerned: (a) Extremely cataclased and corroded arsenopyrite occurs in zone of intensive deformation between black shales and actinolitic schists. Arsenopyrite impregnated the rock along the schistosity and was subject to superimposed deformation. (b) Tiny isolated euhedral crystals of arsenopyrite, often accompanied by stibnite, occur in thin carbonatic veins. These crystals were not affected by deformation and thus represent the youngest generation of arsenopyrite.

Pyrite of hydrothermal origin forms subhedral, scarcely euhedral crystals and their aggregates, often intergrown with cataclased arsenopyrite (Fig. 11). Age relations in such aggregates are ambiguous and crystallization intervals of the two minerals seem to overlap. Aggregates with gudmundite were observed as well. (Fig. 11). Pyrite grains often enclose quartz and carbonate inclusions. Typical is slight optical anisotropy of pyrite due to admixture of As, zonality is rare. The Au contents of up to 10 ppm were detected in pyrite (see analyses in table 3).

Gudmundite is rather abundant ore mineral in the samples from the Trojárová adit. We distinguished two generations. Gudmundite-I occurs as disseminated clusters of subhedral and anhedral crystals in arsenopyrite and arsenopyrite-pyrite aggregates or it forms monomineral aggregates and veins in pyrite and arsenopyrite (Fig. 11). It often encloses relict grains and fragments of arsenopyrite. Pyrrhotite either penetrates into gudmundite aggregates (Fig. 12) or occurs along with gudmundite as isolated clusters in carbonates. Gudmundite-I is usually present in boundary zones of carbonatic veins with Sb-mineralization (Fig. 13), where it directly contacts quartz crystals and often also pyrrhotite. Gudmundite II associates with stibnite, berthierite, native Sb or with Sb oxides/sulphooxides. Cataclased gudmundite is often replaced by stibnite. Admixtures of other elements were not detected (Tab. 4, analyses 1-3).

Pyrrhotite occurs in two morphological types. 1. Veins of pyrrhotite intrude into the arsenopyrite-gudmundite aggregates (Fig. 12). 2. Pyrrhotite of younger generation is euhedral or subhedral, occurs as a component of carbonate veins, where it is accompanied by berthierite and native antimony (Fig. 14), intergrows with native antimony (Fig. 15) or gudmundite (Fig. 16), rarely with arsenopyrite (Fig. 17). The mineral pairs gudmundite–pyrrhotite, resp. native antimony–pyrrhotite exhibit equilibrium microstructures. On the other hand, pyrrhotite is intensively replaced by stibnite (Fig. 16) and berthierite, often even pseudomorphed by the later.

Slovak Geol. Mag., 8, 3– 4 (2002), 179 – 193

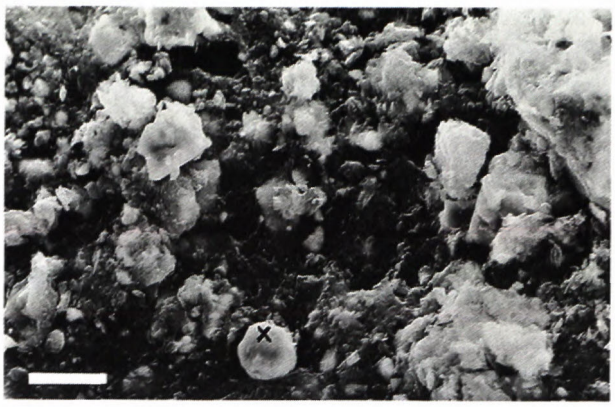

Fig. 6

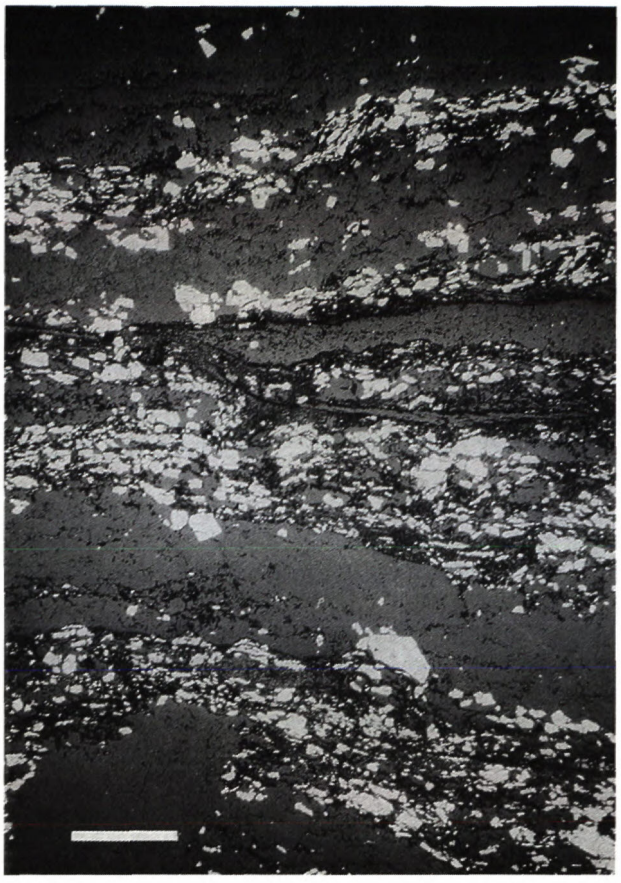

Fig. 7

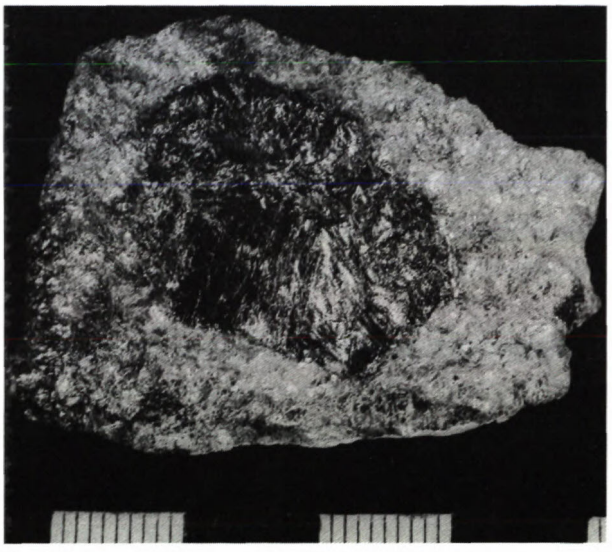

Fig . 8

Fig. 9

Fig. 10

Fig. 6 Morphology of graphite from the concentrate, graphite grain is marked with character "x", SEM image, scale bare corresponds to 10 μm.

Fig. 7 Typical texture of synsedimentary pyrite (white) from pyrite-pyrrhotite mineralization in black shales of Trojárová deposit, reflected light, scale bar is 500 μm.

Fig. 8 Crystal of molybdenite from greisenized granite, borehole sample PT 45/271.1. 1 unit is 1 cm.

Fig. 9 Irregular sectorial zonation of inhomogeneous, cataclased arsenopyrite grains in black quartz from the first stage of hydrothermal mineralization, SEM image, scale bar is 100 μm.

Fig. 10 Typical laminar zonation of fine-grained euhedral arsenopyrite, the first stage of hydrothermal mineralization, SEM image, scale bar is 10 μm.

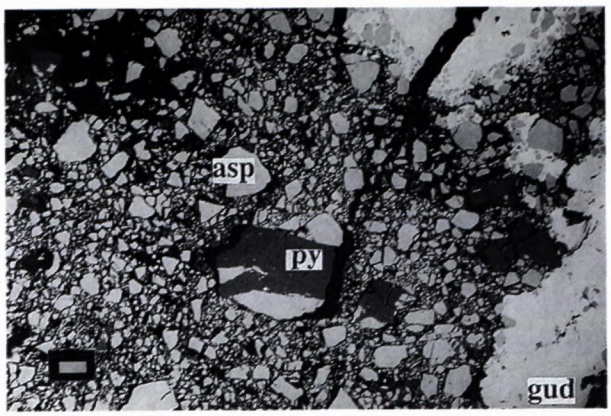

Fig. 11

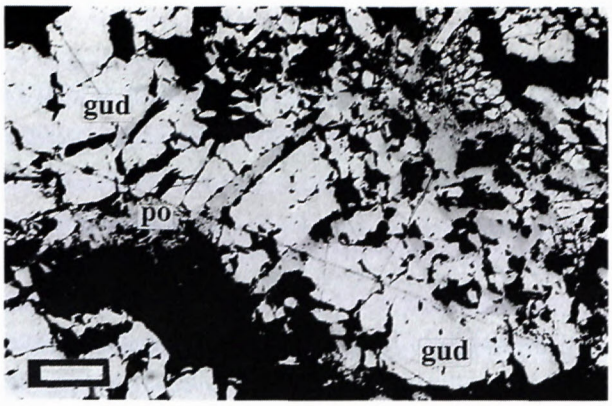

Fig. 12

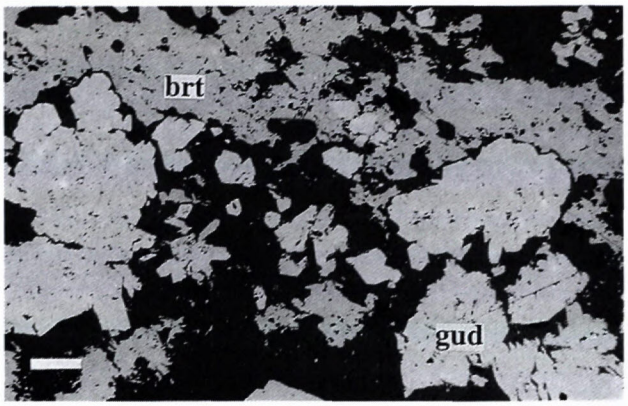

Fig. 13

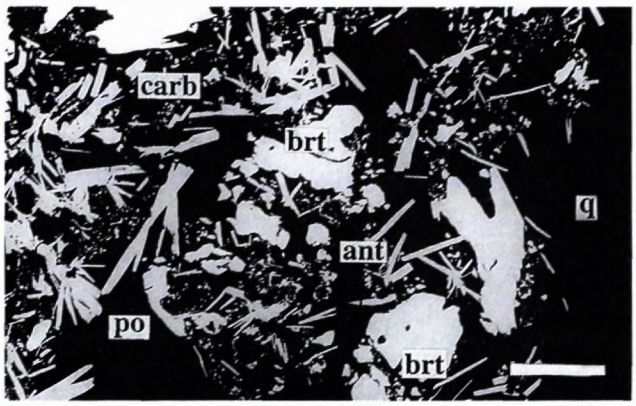

Fig. 14

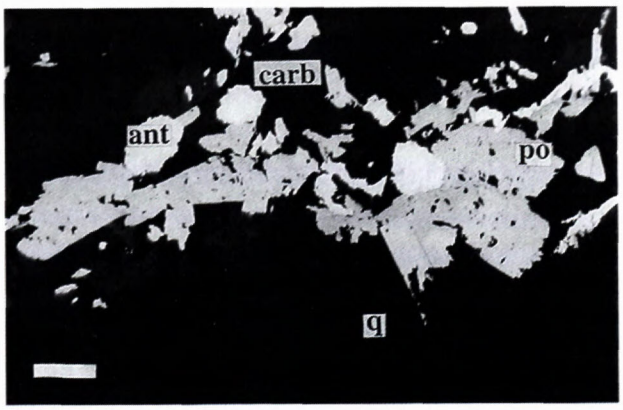

Fig. 15

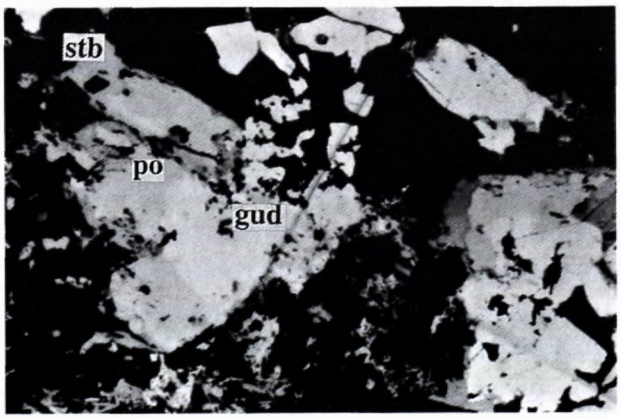

Fig. 16

Fig. 11 Sample with gudmundite (gud) penetrating the arsenopyrite (asp) - pyrite (py) aggregate affected by cataclasis, SEM image, scale bar is 100 μm.

Fig. 12 Reflected light microphotograph of pyrrhotite (po) penetrating the brecciated gudmundite (gu) aggregate, scale bar is 100 μm.

Fig. 13 Vein of younger berthierite (brt) penetrating the gudmundite (gud) aggregate of older stage, borehole sample PT - 52/7, reflected light, scale bar is 100 μm.

Fig. 14 Reflected light microphotograph of relationship between of needle-shape pyrrhotite (po), berthierite (brt) and fine aggregates of native antimony (ant) in a carbonate (carb) vein penetrating voids in quartz (q) aggregate, borehole sample PT – 57/137.4. SEM image, scale bar is 100 μm.

Fig. 15 Textural relationship between pyrrhotite (po) and native antimony (ant) in carbonate vein (carb), ore minerals are in sharp contact. This mineralization is in contact with older quartz crystals (q), scale bar is 100 μm (reflected light).

Fig. 16 Intergrowth of pyrrhotite (po) and gudmundite (gud) – an equilibrium association, stibnite (stb) replaces the pyrrhotite, reflected light, scale bar is 100 μm.

Slovak Geol. Mag., 8, 3–4 (2002), 179 – 193

Tab. 3 Electron microprobe analyses of arsenopyrite (wt.%), the Pezinok – Trojárová deposit.

Analyse number	1	2	3	4	5	6	7	8	9	10	11	12	13	14
Sample	T-24	T-24	T-24	T-24	T-39	T-39	T-39	T-20A	T-29	T-29	T-29	T-30	T-30	T-30
Fe	33.19	33.18	34.16	33.83	35.35	35.18	35.69	35.61	35.09	34.31	35.87	36.81	35.60	36.03
Sb	0.04	0.06	0.07	0.06	0.00	0.00	0.00	1.52	1.12	0.35	0.99	0.00	0.41	0.00
Bi	0.13	0.12	0.03	0.07	0.00	0.00	0.00	0.00	0.00	0.00	0.04	0.00	0.00	0.00
S	22.08	23.17	21.46	22.89	22.64	23.97	22.93	20.05	24.58	23.71	23.45	22.30	24.99	23.92
Au	0.67	0.54	0.04	0.00	0.00	0.00	0.00	0.01	0.00	0.00	0.00	0.00	0.00	0.00
As	42.06	41.69	42.80	42.25	41.30	40.14	41.18	42.73	38.46	41.19	39.87	41.80	39.42	40.63
Ni	0.15	0.00	0.24	0.00	0.00	0.00	0.00	0.00	0.00	0.00	0.00	0.00	0.00	0.00
Co	0.00	0.00	0.00	0.00	0.00	0.00	0.00	0.00	0.00	0.00	0.00	0.00	0.00	0.00
Σ	98.32	98.76	98.80	99.10	99.29	99.29	99.80	99.92	99.24	99.55	100.22	100.91	100.42	100.58
	recaltulated on the 3 of atoms													
Fe	0.96	0.95	0.99	0.96	1.00	0.99	1.01	1.04	0.98	0.97	1.01	1.03	0.98	1.00
Sb	0.00	0.00	0.00	0.00	0.00	0.00	0.00	0.02	0.01	0.00	0.01	0.00	0.01	0.00
Bi	0.00	0.00	0.00	0.00	0.00	0.00	0.00	0.00	0.00	0.00	0.00	0.00	0.00	0.00
S	1.12	1.16	1.08	1.14	1.12	1.17	1.13	1,02	1.20	1.16	1.15	1.09	1.2	1.16
Au	0.01	0.00	0.00	0.00	0.00	0.00	0.00	0.00	0.00	0.00	0.00	0.00	0.00	0.00
As	0.91	0.89	0.92	0.90	0.87	0.84	0.87	0.93	0.80	0.87	0.83	0.88	0.81	0.84
Ni	0.00	0.00	0.00	0.00	0.00	0.00	0.00	0.00	0.00	0.00	0.00	0.00	0.00	0.00
Co	0.00	0.00	0.00	0.00	0.00	0.00	0.00	0.00	0.00	0.00	0.00	0.00	0.00	0.00

Stibnite is a component of carbonate veins cutting the arsenopyrite-pyrite paragenesis and filling fractures in cataclased arsenopyrite and pyrite crystals. These veins also penetrate into surrounding actinolithic shales. The contents of stibnite is generally low. Several textural types were determinated:

1. Massive monomineral stibnite aggregates show evidences of superimposed dynamic recrystallization, such as deformation twins, shape-preferred orientation and even features of crystallographically preferred orientation of aggregates. Stibnite encloses quartz and older gudmundite with signs of corrosion and replacement. Stibnite of this type often intergrows with massive native antimony, however, their contact is rarely direct – Sb oxides/sulphooxides occur as an interface instead. (This applies mostly on the Antimonitová adit samples, Kolársky vrch). Stibnite associates with pyrrhotite and berthierite (Fig. 14) and also occurs in mixtures of Sb oxides/sulphooxides, probably as a relict (Fig.18).
2. The vein-filling stibnite, (likewise berthierite), often replaces pyrrhotite in its aggregates with gudmundite or with native antimony (Fig. 16, 17, respectively). Sometimes stibnite was observed to cement aggregates of these minerals.
3. Radial stibnite aggregates crystallized in cavities of Sb oxides/sulphooxides as well as along fissures in the host rock likely represent the youngest stibnite generation remobilized in the latest mineralization stage. The thin stibnite veins often seal hydraulically brecciated oxide aggregates. Stibnite identification was confirmed by electron microprobe analyses (Tab. 4, analyses 4-6).

Berthierite is rare and it's occurrence is related to Sb mineralization in carbonate veins (Fig. 14). It forms thin veinlets in pyrrhotite, sometimes also monomineral aggregates. Berthierite replaces and pseudomorphs pyrrhotite. In its intergrows with tetraedrite and arsenopyrite berthierite forms cores of these aggregates. Berthierite is more abundant in association with stibnite and kermesite within carbonates, where it forms veins and spicular crystals (Tab. 4, analyses 7 and 8).

Native antimony is scarce, it seldom occurs in larger clusters of anhedral isometric grains or aggregates with mosaic structure (Fig. 14, 15, Tab. 4, analysis 9). Significant accumulations of native antimony were observed in samples from the Antimonitová adit (Kolársky vrch deposit), where it often dominates over Sb sulphides and forms massive monomineral aggregates. Study of the Trojárová locality supplemented by the samples from Kolársky vrch deposit, revealed, that native antimony, accompanied by pyrrhotite, gudmundite, berthierite and stibnite, is a component of carbonatic mineralization. Native antimony intergrows with pyrrhotite, forming equilibrium microstructures. It is frequently corroded and replaced by kermezite, valentinite and senarmontite, which commonly occurs along the boundaries with quartz grains.

Galenite and *sphalerite* are very rare. Galenite seals the fissures in *sphalerite* aggregates. Fe contents in the sphalerite is about 5 wt. % (Tab. 4, analysis 11). It also associates with gudmundite and pyrrhotite.

Chalcopyrite, as very rare mineral, occurs in parageneses with tetrahedrite and gudmundite or it forms individual anhedral grains in carbonate veins, which penetrate into cataclased arsenopyrite-pyrite aggregates.

Tab. 4 Electron microprobe analyses of minerals of stibnite mineralization (wt. %), the Pezinok – Trojárová deposit, gudmundite (1-3), stibnite (4-6), berthierite (7, 8), native antimony (9), galena (10), sphalerite (11), tetrahedrite (12), pyrite (13, 14).

Analyse number	1	2	3	4	5	6	7	8	9	10	11	12	13	14
Sample	T-39	45/8	45/8	36/10	45/2	T-20A	57/171.9	45/8	57/137.4	11/139.8	11/139.8	45/8	T-39	T-30
Fe	28.32	24.39	25.39	0.21	0.02	0.24	12.54	12.67	0.24	0.03	5.83	5.92	46.96	45.66
Sb	55.77	61.52	60.15	73.27	73.65	73.36	58.57	58.51	99.98	-	-	31.86	0.00	0.00
Bi	-	0.03	-	-	0.22	-	0.80	-	0.00	-	-	-	0.00	0.00
S	16.56	15.27	15.54	26.88	25.28	27.80	28.97	28.49	0.02	12.98	31.84	25.41	54.92	53.02
Au	0.00	-	-	-	-	0.00	-	-	-	-	-	-	0.00	0.00
As	0.00	0.35	-	-	0.12	0.00	0.02	0.70	0.00	-	-	-	0.00	2.55
Ni	-	-	-	0.02	-	-	-	0.02	-	-	-	-	0.00	0.00
Co	-	0.02	-	0.01	0.03	-	-	-	-	-	-	-	0.00	0.00
Cu	-	0.14	-	-	0.02	-	-	0.15	-	-	-	36.98	-	-
Zn	-	-	-	0.01	0.01	-	-	-	-	0.09	61.08	0.80	-	-
Hg	-	0.06	-	0.33	0.19	-	0.32	0.09	0.38	-	-	0.71	-	-
Mn	-	-	-	-	-	-	-	-	-	0.07	0.03	-	-	-
Cd	-	-	-	-	-	-	-	-	-	0.03	0.45	-	-	-
Ag	-	0.02	-	0.05	0.01	-	-	0.02	-	0.04	-	0.07	-	-
Pb	-	-	-	-	-	-	-	-	-	86.61	-	-	-	-
Σ	100.71	101.80	101.08	100.78	99.55	101.40	101.22	100.65	100.62	99.85	99.23	101.75	101.89	101.22
recaltulated on the Σ of atoms	3	3	3	5	5	5	7	7	-	2	2	29	3	3
Fe	1.02	0.92	0.95	0.01	0.00	0.01	0.97	0.99	-	0.00	0.10	1.83	0.99	0.98
Sb	0.93	1.07	1.03	2.11	2.16	2.04	2. 09	2.09	-	-	-	4.33	0.00	0.00
Bi	-	0.00	-	-	0.00	-	0.02	-	-	-	-	-	0.00	0.00
S	1.04	1.01	1.01	2.88	2.82	2.94	3.92	3.87	-	0.98	0.98	13.17	2.01	1.98
Au	0.00	-	-	-	-	0.00	-	-	-	-	-	-	0.00	0.00
As	0.00	0.00	-	-	0.12	0.00	0.23	0.04	-	-	-	-	0.00	0.04
Ni	-	-	-	0.00	-	-	-	0.00	-	-	-	-	0.00	0.00
Co	-	0.00	-	0.00	0.00	-	-	-	-	-	-	-	0.00	0.00
Cu	-	0.00	-	-	0.00	-	-	0.01	-	-	-	9.67	-	-
Zn	-	-	-	0.00	0.00	-	-	-	-	0.09	0.92	0.16	-	-
Hg	-	0.00	-	0.00	0.00	-	0.01	0.00	-	-	-	0.00	-	-
Mn	-	-	-	-	-	-	-	-	-	0.00	0.00	-	-	-
Cd	-	-	-	-	-	-	-	-	-	0.00	0.00	-	-	-
Ag	-	0.00	0.00	0.00	0.00	-	-	0.00	-	0.00	-	0.00	-	-
Pb	-	-	-	-	-	-	-	-	-	1.01	-	-	-	-

Slovak Geol. Mag., 8, 3–4 (2002), 179 – 193

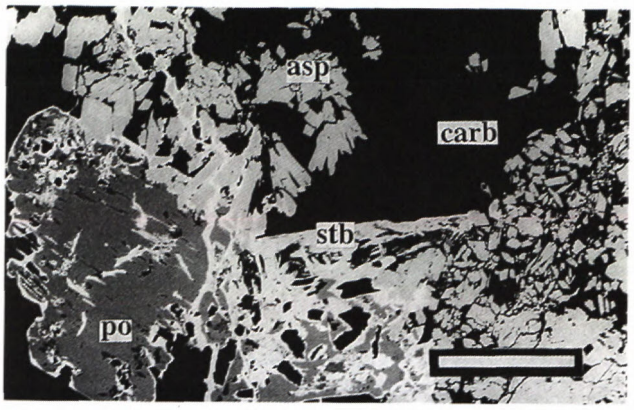

Fig. 17 Pyrrhotite (po), arsenopyrite (asp), stibnite (stb) in carbonate (carb) vein. Pyrrhotite is replaced by stibnite, arsenopyrite appears to be in equilibrium with pyrrhotite, adit sample, SEM image, scale bar is 100 μm.

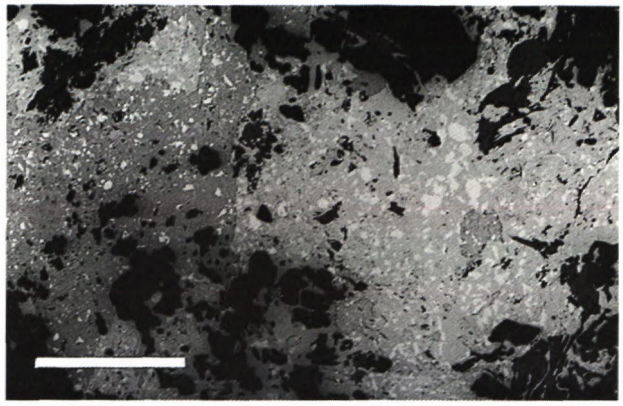

Fig. 18 SEM image of replacement texture of hypogene kermesite (dark grey), valentinite (grey) and native antimony (white), scale bar is 100 μm.

Tetrahedrite is rare, it associates with chalcopyrite, berthierite, eventually with native antimony. From the chemical composition follows its classification as an Sb member of the tetrahedrite-tenantite series with minor As contents and increased Fe contents. Contents of Zn, Hg, and Ag are low (Tab. 4, analysis 12).

Ullmanite was recorded in calcite veins with gudmundite, chalcopyrite, tetrahedrite, and berthierite. Detailed description and data for this mineral are summarised in Andráš & Chovan (1995).

Gold is chemically bonded preferentially to arsenopyrite and pyrite with contents up to 230 ppm (Andráš et al., 1995, 2000). Its distribution is irregular and Au bonding in sulphides is not satisfactorily explained. No visible gold was recorded on the Trojárová deposit.

Sb oxides and sulphooxides represent a unique stage in the Sb-Fe-As-Au mineralization, characterized by shift from sulphidic towards oxidic conditions. Abundant *kermesite* forms aggregates or spicular crystals, often radially arranged. In massive ores it intergrows with stibnite and also associates with gudmundite, berthierite and native antimony. Kermesite also forms intergrowths with other Sb oxides/sulphooxides (Fig. 18). *Valentinite* was identified optically and microchemically (Tab. 5, analyses 2, 3). *Senarmontite* is isotropic and intergrows with kermesite and valentinite. *Cervantite* was also identified macroscopically. Sb oxides/sulphooxides replace native antimony and stibnite, especially along boundaries between the two minerals or along their boundaries with quartz. Relics of the primary phases often occur in the aggregates of Sb oxides/sulphooxides (Fig. 18). Aggregates of Sb oxides/sulphooxides were intersected by veins of younger generation of stibnite, which has also sealed hydraulic fractures in these aggregates (samples from Antimonitová adit, Kolársky vrch).

Gangue minerals

Carbonates are dominant gangue minerals on the Trojárová deposit. They form lenses and veins in black shales of thickness ranging from centimetres up to several decimetres but rarely they also occur in adjacent "actinolitic" schists and amphibolites. Fine- to medium grained carbonate aggregates of grey or yellowish-white colour are usually intergrown with quartz and host As-, Sb-, and Fe-sulphides. According to DTA and manometric analyses dolomite-ankerite predominate, calcite is more seldom. The younger (several mm thick) carbonate veins of white colour, intersecting older massive carbonatic aggregates and upright penetrating the schistosity, consist exclusively of calcite. Marcasite is present in these calcite veins.

Quartz accompanied by arsenopyrite and pyrite forms cataclased lenses and short veinlets in black shales. Quartz of younger generation, associated with Sb sulphidic mineralization, occurs very rarely.

Discussion and conclusions

Trends of enrichment factors of metallic elements in ore-bearing black shales of the Trojárová deposit are similar to those in other productive zones in wider Pezinok area. This concerns mainly C_{org}, C_{min}, As, Sb, Au, S, Mo, and V. High contents of S is due to intensive pyritization in black shales and surrounding rocks. The contents of Sb, Au and As in black shales are markedly increased in comparison with weekly altered and unaltered rocks. Variations in the S concentration depend on the intensity of pyritization. Sb and As enrichments in black shales are negligible and show negative correlation with C_{org}. As, Sb, and S contents are slightly increased in hydrothermally altered rocks.

Correlation relations between elements indicate 1) binding of Au to arsenopyrite; 2) close association of ore minerals with carbonates and 3) intensive pyritization of black shales. Since the Sb mineralization is hosted in carbonate veins, often cutting the black shale foliation, it is considered as epigenetic. However, significant positive correlation of Sb and C_{org} and weak negative correlation of Sb and C_{min} in 12 samples from boreholes (Fig.4) contradict to this statement. The explanation is problematic. Macroscopical crystals of Sb minerals and their variable

Tab. 5 Electron microprobe analyses of molybdenite (1) and Sb oxides (2,3) and sulphooxides (4-6), the Pezinok – Trojárová deposit.

Analyses number	1	2	3	4	5	6
Sample	45/271	57/171.9	57/171.9	57/171.9	57/171.9	57/171.9
As	-	0.10	0.00	0.00	0.17	0.00
Bi	-	0.00	0.05	0.39	0.00	0.00
Fe	-	0.01	0.03	1.47	0.00	1.13
Hg	-	0.61	0.00	0.90	0.17	0.41
Mo	60.54	-	-	-	-	-
S	39.20	0.09	0.03	20.14	18.68	18.37
Sb	-	80.22	80.51	73.18	74.99	73.72
W	0.20		-	-	-	-
Σ	99.94	81.03	80.62	96.08	94.01	93.63
Recalculated on	2 atoms	3 oxygens	3 oxygens	1 oxygen	1 oxygen	1 oxygen
Mo	1.02	-	-	-	-	-
S	1.98	-	-	2.16	1.88	1.85
Sb	-	1.78	1.79	2.07	1.99	1.96
O	-	3.20	3.27	0.84	1.20	1.23
Σ	-	4.98	5.06	5.07	6.07	6.04

content in carbonate veins can devalue results of statistical analysis. Association of Sb minerals with carbonate veins was confirmed by statistical analysis of 42 samples from borehole, with positive correlation between C_{min} and Sb (r = 0.51) (Chovan et al., 1990), as well as in samples of black shales form Trojárová adit (Fig. 5).

Three ore mineralizations types were distinguished (Table 6). The oldest *exhalation-sedimentary pyrite* mineralization has evolved in black shales and was subsequently metamorphosed. Dominant association pyrite-pyrrhotite is accompanied by accessory chalcopyrite and sphalerite. In the same environment the later superimposed *hydrothermal Sb-Fe-As-Au* mineralization took place. The occurence of the *molybdenite mineralization* is restricted to the leucogranite.

Arsenopyrite is the most abundant ore mineral in samples of hydrothermal mineralization from the Trojárová deposit, pyrite is less frequent. Gudmundite, pyrrhotite and stibnite are rather abundant in samples from Sb-mineralization. Sphalerite, berthierite, native antimony, tetrahedrite, chalcopyrite, and ullmanite are rare. The Au- enrichment was detected in all textural varietes of arsenopyrite and pyrite. Pyrite from surrounding rocks is depleted in Au. Native gold does not occur. Gangue minerals involves predominantly ankerite, minor calcite and quartz.

Despite that complete succession scheme could not be figured out, five evolution periods of hydrothermal mineralization were discerned (see Table 6). The Sb-Fe-As-Au mineralization encompasses several mineral stages.

Pyrite-arsenopyrite stage (1st stage, table 6) associates with carbonates and with dark quartz. Low As contents in studied arsenopyrites does not permit application of the arsenopyrite geothermometer of Kretschmar & Scott (1976), nevertheless, analogical samples from the Kolársky vrch deposit yielded temperature ranges 350-410 °C and 350-450 °C (using geothermometers of Kretschmar & Scott, 1976 and Sundblad et al., 1984, respectively) for crystallization of arsenopyrite (published in András & Horváth, 1985, András et al., 1999). Increased influx of Sb in the 3rd stage probably caused the observed anomalous Sb contents in arsenopyrite.

Younger **gudmundite I** (2nd stage, table 6) often penetrates the pyrite-arsenopyrite aggregates. Such mineral association is stable at increased fS_2 or increased fO_2 (Williams-Jones & Normand, 1997).

Other mineralization stages are characteristic by intensive carbonatization and presence of Sb minerals.

Paragenesis **gudmundite–berthierite–pyrrhotite–native antimony–stibnite** (3rd stage, table 6) is abundant in a carbonatic veinstone from boreholes. Carbonate veins with Sb sulphides and veins with pyrrhotite intensively penetrate the arsenopyrite and arsenopyrite-pyrite aggregates. Pyrrhotite frequently intergrows with gudmundite or with native antimony. **Pyrrhotite** coexists in a stable association with **native antimony**, which is a rather uncommon. According to Borodaev et al. (1985) and Williams-Jones & Normand (1997) such association is stable at high temperatures (Fig. 19). Other example of similar textural relations between the two minerals is described from the stibnite deposit Quebec Antimony in Canada (Normand et al., 1996). The observed association **pyrrhotite-gudmundite**, which also appears in textures indicating a stable coexistence, is, on the contrary, stable at lower temperatures than pyrrhotite-native antimony paragenesis (Fig. 19).

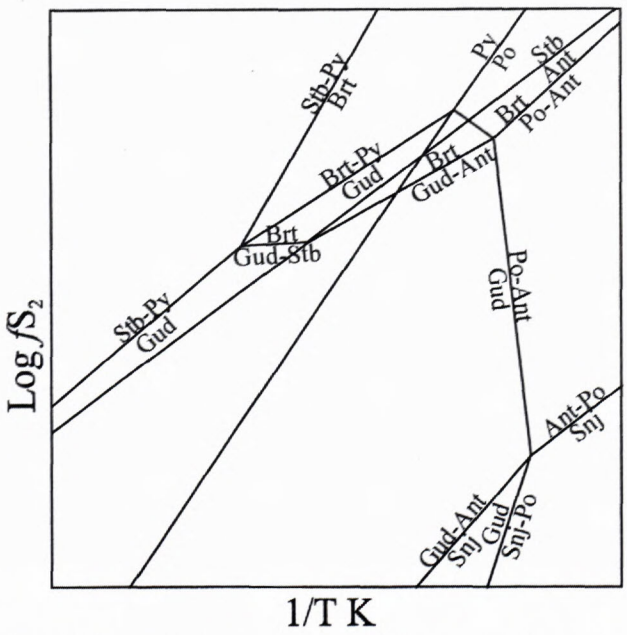

Fig. 19 Topology of the system Fe-Sb-S among the phases stibnite (Stb), native antimony (Ant), gudmundite (Gud), berthierite (Brt), seinäjokite (Snj), pyrite (Py) and pyrrhotite (Po). (After Williams-Jones and Normand 1997).

Pyrrhotite of both associations (with gudmundite and with native antimony, respectively) is intensively replaced by stibnite and berthierite. According to phase diagrams of the system Fe-Sb-S-O proposed by Williams-Jones & Normand (1997) this phase transition indicates a decrease of temperature (Fig. 19).

Tab. 6 Succession, mineral assemblages and elements addition, the Pezinok – Trojárová deposit

MINERALIZATION	MINERAL ASSAMBLAGES	ELEMENTS
metamorphosed exhalation-sedimentary	**pyrite, pyrrhotite**, sphalerite, chalcopyrite	Fe, S
hydrothermal in granitoids	**molybdenite**	Mo, S
hydrothermal Sb-Fe-As-Au in black shales, stages:		
1.	ankerite, calcite, quartz **arsenopyrite and pyrite** with invisible gold	Ca, Mg S, As, Fe, Au
2.	gudmundite I, pyrrhotite I, pyrite, quartz	Sb, Fe, S Si, O
3.	ankerite, calcite pyrrhotite II, native antimony, **gudmundite** II, berthierite, **stibnite I,** kermesite, valentinite, uullmanite, tetrahedrite, chalcopyrite	Ca, Mg, C S, Sb, Fe, Ni, Cu, O
4.	stibnite II, (arsenopyrite, gudmundite) (recrystallised)	As, Fe, Sb, S
5.	**calcite**, marcasite	Ca, C, O, Fe, S

Gudmundite appears to have coexisted stably with berthierite. Gudmundite crystallizes at relatively wide spread of fS_2, however, its association with berthierite is stable at higher values of fS_2 (Fig. 19, Williams-Jones & Normand 1997). On the contrary, overgrowths of gudmundite with stibnite show features of corrosion.

In our samples berthierite is far less abundant than stibnite. Williams-Jones & Normand (1997) explained that if cooling is a controlling factor of mineral deposition, at the state of unbuffered fO_2 (resp. fS_2) berthierite is replaced by stibnite on the cooling path.

Mineral association **stibnite-hypogene kermesite–valentinite-senarmontite** is stable at increased fO_2 and high Sb activity (Williams-Jones & Normand,1997). However, the coeval crystallization of stibnite and Sb oxides / sulfooxides is not evident from textures. The native antimony, stibnite of the 3rd stage (see Table 6), berthierite and gudmundite occur as relics after oxidation in hypogene Sb oxides/sulfooxides. The occurence of native antimony was previously commented by Cambel (1959) who considered it as a transition element on the oxidation path from gudmundite to Sb oxides/ sulfooxides.

The recrystallised euhedral arsenopyrite, tetrahedrite, chalcopyrite and ullmanite are probably connected with 3rd stage (Table 6) mineralization stage.

Late stage stibnite – stibnite II (4th stage, table 6) (thin veinlets, radial aggregates and cements in aggregates of Sb oxides/sulfooxides) appears to be younger than Sb oxides/sulfooxides and coexist with them in a direct contact. It fills fissures and cavities in the Sb oxides/ sulfooxides and native antimony, often crystallized along boundaries between quartz and massive native antimony. The youngest recrystallised stibnite fills the fissures in host rocks. According to Williams-Jones & Normand (1997) stibnite formation is favored by reductive conditions in a course of cooling.

Mineral associations on the deposit Trojárová are analogous to those on the Quebec Antimony deposit, Canada (Williams-Jones & Normand, 1997) where gudmundite and native antimony are dominant ore minerals (Normand et al., 1996) and probably experienced similar evolution, comparable also with other Sb deposits, such as Mari Rosa and El Juncalón deposits in Spain (Ortega & Vindel, 1995), deposits in Montagne Noire region, France (Munoz & Shepherd, 1987), or the Moretons Hratbour deposit in Canada (Kay & Strong, 1983). According to Williams-Jones & Normand (1997) the main factor controlling the stibnite deposition is decreasing temperature.

Acknowledgements: This research was funded the following grants: Economic contract No. 318/89-88/VČ, grant project "Pezinok-Trojárová" II VHČ 72/1993, VEGA 1/5218/98 and VEGA 1/8318/01.

References

Andráš P., 1984: Questions of antimonite and gold mineralization on the Pezinok deposit. Manuscript, GÚ SAV, Bratislava 154 (in Slovak).

Andráš P., Dubaj D.& Kotulová J., 1999: Arsenopyrite geothermometer application at Pezinok Sb-Au deposit. Miner. Slovaca, 31, 322-324 (in Slovak).

Andráš P. & Horvát I., 1985: Thermoanalytical study of the metamorphism grade in Malé Karpaty Mts. region. Geol. Zbor. Geol. Carpathica, 36, 1, 75-84.

Andráš P. & Chovan M., 1995: Ullmanite from the Trojárová deposit (Malé Karpaty Mts.). Miner. Slovaca 27, 75-77 (in Slovak).

Andráš P., Chovan M., Stankovič J., Paulínyová E. & Svitáčová A., 2000: Distribution of "invisible gold" in gold-bearing sulphides from the West Carpathians Tatrikum, Sovakia, Uhlí Rudy, 2, 16-25 (in Slovak).

Andráš P., Wagner F., Ragan M., Friedl J., Marcoux E., Caňo F. and Nagy G., 1995: Gold in arsenopyrites from the Pezinok deposit (W.Carpathians, Slovakia). Geol. Carpathica, 46, 6, 335-342.

Borodaev Y. S., Mozgova N. N., Ozerova N. A., Slusarev V., Oivanen P & Yletyinen V., 1985: Typomorphic mineral associations of antimony deposits with native antimony in the Baltic Shield. Geol. zbor. (Bratislava), 36, 305-313.

Cambel B., 1959: Hydrotermal deposits in the Malé Karpaty Mts. - mineralogy and geochemistry of their ores. Acta Geol. Geogr. Univ. Comenianae (Bratislava), 3, 338.

Cambel B., Miklós J., Khun M. & Veselský J., 1990: Geochemistry and petrology of clay-metamorphic rocks of the Malé Karpaty Mts. Crystalline complex. Geol. Instit. Slovak. Acad. Sci., Bratislava, 1-267.

Cambel B. & Khun M., 1983: Geochemical characteristic of black shales from the ore-bearing complex of the Malé Karpaty Mts. Geol. Zbor. – Geol. Carpath., 34, 1, 15-44.

Cambel B. & Vilinovič V.,1987: Geochemistry and petrology of granitoids of Malé Karpaty Mts. Veda, Bratislava, 248 (in Slovak).

Ďurža O. & Chovan M., 1995: Thermoelectrical power of molybdenite from Western Carpathian granitoid massives. Miner. Slovaca, 27, 283-286 (in Slovak).

Hanas P., Stupák J. & Tréger M., 1989: The preliminary report Pezinok - Trojárová. Manuscript, Geofond, Bratislava, 101 (in Slovak).

Chovan M. (ed.), 1990: Mineralogical, geochemical and petrographical study of borehole on the Pezinok-Trojárová deposit. Manuscript, Comenius University, Bratislava, 119 p. (in Slovak).

Chovan M., Rojkovič I., Andráš P. & Hanas P., 1992: Ore mineralization of the Malé Karpaty Mts. Geol. Carpathica, 43, 275-286.

Janků H., 1991: Graphite in the Pezinok - Pernek crystalline complex. Manuscript, PriF UK, Bratislava, 59 (in Slovak).

Judovič J. E., Ketris M. P. & Merc A. V., 1990: Geochimija i rudogenez zolota v čornych slancach. IGCP 254, Syktyvar, 61.

Judovič J. E. & Ketris M. P., 1991: Geochimija i rudogenez toksičnych elementov - primesej (Cd, Hg, As, Sb, Se) v čornych slancach. IGCP 254, Syktyrkar, 80.

Kantor J., 1974: Sulphur isotopes of the stratiform pyrite deposit Turecký vrch and stibnite deposit Pezinok, in Malé Karpaty Mts. crystalline, Czechoslovakia. Geol. Zbor. SAV, 25, 2, 331 - 334.

Kay A. & Strong D.F., 1983: Geologic and fluid controls on As-Sb-Au mineralization in the Moretons Harbour area, Newfoundland. Econ. Geol., 78, 1590-1604.

Korikovskij S. P., Cambel B., Miklóš J. & Janák M., 1984: Metamorphose of the Malé Karpaty Mts. crystalline: stages, zonality, connection with the granitoids. Geol. Zbor. Geol. Carpathica, 35, 4, 437-462 (in Russian).

Kretschmar U. & Scott S. D., 1976: Phase relation involving arsenopyrite in the system Fe-As-S and their application. Canad. Mineralogist, 14, 363-386.

Leake B.E., Woolley A.R., Arps Ch.E.S., Birch W. D., Gilbert M. Ch., Grice J.D., Hartworne F. C., Kato A., Kisch H.J., Krivovichet V.G., Linthout K., Laird J., Mandarino J. A., Maresch W.V., Nickel E.H., Rock N. M.S., Schumacher J.C., Smith D.C., Stephenson N. C. N., Ungaretti L., Whittaker E.J.W. & Youzhi G., 1997: Nomenclature of amphibolites: report of the subcommitee on amphiboles of the international mineralogical association, commission on new minerals and mineral names. The Canadian Mineralogists, 35,219-237.

Maheľ M., 1983: Beziehung Westkarpaten-Ostalpen, Position der Ubergangs-Abschnites-Deviner Karpaten. Geol. Zbor. Geol. Carpathica, 34, 2, 131-149.

Moravanský D., 2000: Chemical composition of selected minerals and it´s changes in hydrotermal alteration processes of γδ and metahasites (philosilicates and amphibolites). Manucript, RNDr. thesis, PriF UK, Bratislava, 74.

Moravanský D., Chovan M. & Lipka J., 2001: Phyllosilicates form hydrothermally altered granitoid rocks in the Pezinok Sb-Au deposit, Western Carpatians, Slovakia. Geol. Carpathica, 52, 3, 127-138.

Munoz M. & Shepherd T. J., 1987: Fluid inclusion study of the Bournac polymetallic (Sb-As-Pb-Zn-Fe-Cu...) vein deposit (Montagne Noire, France). Mineral. Deposita, 22, 11-17.

Normand CH., Gauthier M. & Jébrak M,. 1996: The Québec Antimony Deposit: An Example of Gudmundite-Native Antimony Mineralization in the Ophiolitic Mélange of the Southeastern Québec Appalachians. Economic Geology, 91, 149 - 163.

Ortega L. & Vindel E., 1995: Evolution of ore forming fluid associated with late Hercynian antimony deposits in Central/Western Spain: case study of Mari Rosa and El Juncalón. Eur. J. Mineral., 7, 655-673.

Oružinský V., Chovan M. & Hanas P., 1990: Black shales and Sb, Fe mineralization at the Pezinok - Trojárová deposit. Geol. Prusk., Praha, 9/10, 290-291 (in Slovak).

Planderová E. & Pahr A., 1983: Biostratigraphical evaluation of weakly metamorphosed sediments of Wechsel series and their possible correlation with Harmónia Group in Malé Karpaty Mts. Miner. Slovaca, 15, 5, 358-436.

Plašienka D., Michalík J., Kováč M., Gross P. & Putiš M., 1991: Paleotectonic evolution of Malé Karpaty Mts. - an overview. Geol. Carpathica, 42, 4, 195-208.

Polák S., 1974: Antimony ores of the Malé Karpaty Mts. - a new insight into prospecting problematic. Geol. Pruskum, 16, 97-99 (in Slovak).

Polák S. & Rak D., 1980: Prognostication problem of antimony mineralization in the Malé Karpaty Mountains. In: Ilavský (Ed.): Antimony ore mineralizations of Czechoslovakia, GÚDŠ, 69-88 (in Slovak).

Putiš M., 1987: Geology and tectonics of SW and N part of the crystalline in Malé Karpaty Mts. Miner. Slovaca, 19, 2, 135-157 (in Slovak).

Uher P., Chovan M. & Majzlan D., 1994: Vanadian-chromian garnet in mafic pyroclastic rocks of the Malé Karpaty Mts., Western Carpathians, Slovakia. Candian Mineralogist, 32, 319-326.

Sundblad K., Zachrison E., Smers, S. H., Berglund S. & Alinder C., 1984: Sphalerite geobarometry and arsenopyrite geothermometry applied to metamorphoused sulfide ores in the Swedish Caledonides. Econ. Geol., 79, 1660-1668.

Williams-Jones A. E. & Normand Ch., 1997: Controls of Mineral Parageneses in the System Fe-Sb-S-O. Econ. Geol., 92, 308 - 324.